Catalysis Today 149 (2010) 19–27

Contents lists available at ScienceDirect

Catalysis Today

journal homepage: www.elsevier.com/locate/cattod

# Activity and sulfidation behavior of the $CoMo/Al_2O_3$ hydrotreating catalyst: The effect of drying conditions

A.V. Pashigreva *, G.A. Bukhtiyarova, O.V. Klimov, Yu.A. Chesalov, G.S. Litvak, A.S. Noskov

*Boreskov Institute of Catalysis SB RAS, pr. ak. Lavrentiev, 5, Novosibirsk 630090, Russia*

ARTICLE INFO

*Article history:*
Available online 28 August 2009

*Keywords:*
CoMo catalyst
Chelate ligand
Sulfidation

ABSTRACT

The influence of drying condition of the $CoMo/Al_2O_3$ catalyst prepared using citric acid as a chelating agent on the sulfidation behavior and on the catalytic activity to hydrodesulfurization of straight-run gas oil (SRGO) was investigated. The catalysts dried at 110, 220, 300 and 400 °C were studied using Raman, IRS and DTG techniques. The sulfidation behavior with straight-run gas oil spiked with dimethyldisulfide (DMDS) was investigated using gas chromatography (GC) with a thermal conductivity detector and GC with an atomic-emission detector for analysis of gas and the liquid phases, respectively. It was shown that the sulfidation behavior of the catalysts prepared using the chelating agents depends on the drying condition: the lower drying temperature, the later DMDS conversion and oxide precursor sulfidation starts. A higher activity in SRGO desulfurization was obtained with catalysts dried at 110 and 220 °C. This phenomenon was accounted for by the stabilization effect of chelating agent that retards precursor sulfiding but provides favorably the formation of active CoMoS phase and achieving the highest activity.


## 1. Introduction

The ever toughening standards on the content of harmful compounds in exhaust gases of motor vehicles make it necessary to effectuate new specifications for motor fuels. Since 2005 the European fuel regulations require the maximum diesel sulfur content of 50 ppm and require no more than 10 ppm of sulfur after January 1, 2009 [1]. In Russia, the EURO-3 standards (350 ppm of sulfur) came into force on January 1, 2009 and EURO-4 (50 ppm of sulfur) will be put in force on January 1, 2012 [2]. The production of fuel to meet these regulations will need new effective hydrotreatment catalysts.

The conventional catalysts for hydrodesulfurization of diesel fractions are the $Co–Mo/Al_2O_3$ and $Ni–Mo/Al_2O_3$ sulfide systems. It is well accepted that the active component of hydrotreatment catalysts comprises nanosized $MoS_2$ particles with cobalt or nickel atoms decorated their edges and corners; the particles form the so-called Co(Ni)–Mo–S phase [3–11]. Two types of the Co(Ni)–Mo–S phase are described in the literature. The Co(Ni)–Mo–S phase of type I is characterized by the strong interaction with the support due to the formation of Mo–Al–O bonds and by low degree of sulfidizing. In the Co(Ni)–Mo–S phase of type II, the particles are fully sulfidized and only Van der Waals forces hold them on the support surface [4–7,9], the specific activity (per number of Co atoms in the Co–Mo–S phase) of type II phase being considerably higher than the activity of type I [4,10]. The modern catalysts for fine hydrotreatment of diesel fuel are very efficient due to high concentrations of the active components (a disperse Co(Ni)–Mo–S phase of type II) on the alumina surface [11].

Among the methods to form preferably active type II Co(Ni)–Mo–S phase on the support surface is supporting the active components from solutions containing chelate agents [9,12–30]. There are numerous examples reported in the literature on improving the activity of Co(Ni)Mo sulfide catalysts using chelating ligands: nitrilotriacetic, ethylenediaminetetraacetic and cyclohexanediaminetetraacetic acids [9,12–24], citric [24–28] and thioglycolic acids [29,30].

In opinion of some researchers, chelating additives favor the dispersion of active components through the support surface [14–17], diminish the interaction of the active component (Mo) and promoter (Co) with the support to form the type II active sulfide phase [10,18–20]. In addition, in the presence of chelate ligands, sulfidation of Co(Ni) starts at a higher temperature simultaneously with [29,30] or after [12,13,31–35] the formation of Mo sulfide. Such a sulfidation order minimizes the probability of Co segregation into an individual phase and favors its arrangement on side faces of Mo sulfide to give rise to the formation of the active Co–Mo–S phase.

* Corresponding author at: Boreskov Institute of Catalysis SB RAS, Hydrogenation Process Group, pr. ak. Lavrentiev, 5, Novosibirsk 630090, Russia.
Tel.: +7 383 3269410; fax: +7 383 3308056.
*E-mail address:* pav@catalysis.ru (A.V. Pashigreva).

0920-5861/$ – see front matter © 2009 Elsevier B.V. All rights reserved.
doi:10.1016/j.cattod.2009.07.096

It is reported [6,13,17–22,26,33] that the higher activity to hydrodesulfurization is observed when the catalysts prepared using chelate ligands are not calcined before being sulfidized. At the same time, some contrary data are available in literature [36–39]. For example, the calcinations of catalysts, in which NTA was added before the sulfidation, influenced favorably the HDS activity [36]. When calcined, the Co–Mo/MgO–$Al_2O_3$ catalysts prepared with CyDTA as the chelating agent were more active to thiophene hydrodesulfurization [37]. Diammonium ethylenediaminetetraacetate (diA-EDTA) was used as the chelating agent for the preparation of the commercial CoMo on alumina HDT catalysts [38]; the resulting catalyst was more active to tetralin hydrogenation when the preparation procedure included not only drying but also drying and calcination.

To clarify more the influence of the thermal treatment condition on the hydrodesulfurization activity we try to follow the sulfidation behavior of the Co–Mo/$Al_2O_3$ catalysts prepared using citric acid as the chelate ligand with the subsequent drying at the different temperatures: 110, 220, 300 and 400 °C. The conditions of sulfidation (gas or liquid phase, hydrogen pressure) influence considerably the formation of the Co–Mo–S phase [39–41]. While organosulfide compounds are used for activation of commercial hydrotreating catalysts, straight-run oil gas spiked with dimethyldisulfide (DMDS) was used for the studies. Gas chromatograph (GC) equipped with a thermal conductivity detector and an atomic-emission detector was used for analysis of gas and liquid phases, respectively, to understand regularities of the sulfidation.

## 2. Experimental

### 2.1. Preparation of the complexes and catalysts

The bimetallic compound for catalyst preparation was synthesized from the ammonium salt of the tetrameric citrate anion $[Mo_4(C_6H_5O_7)_2O_{11}]^{4-}$, which was prepared via dissolution of 44.8 g (0.234 mol) of citric acid $C_6H_8O_7{\cdot}H_2O$ and 57.92 g (0.328 mol of Mo) of ammonium heptamolybdate $(NH_4)_6Mo_7O_{24}{\cdot}4H_2O$ in a small amount of distilled water, followed by the addition of more water to obtain exactly 200 ml of solution. Adding solid $Co(CH_3COO)_2{\cdot}4H_2O$ to the solution containing ammonia salt of $[Mo_4(C_6H_5O_7)_2O_{11}]^{4-}$ anion in proportions equivalent to a Mo/Co = 2 atomic ratio, $Co_2[Mo_4(C_6H_5O_7)_2O_{11}]$ was obtained [42,43]. The resulting solution, under ethanol precipitation gave a rose-colored powder of $Co_2[Mo_4(C_6H_5O_7)_2O_{11}]$.

Catalysts were prepared by impregnating alumina granules with a solution of CoMo complex. γ-$Al_2O_3$ granulated in the form of trilobe extrudates with diameter of 1.4 mm and length/diameter ratio equal to 3–5 (from JSK "Promkataliz", Ryazan) was used as the support. The specific surface area of 285 $m^2/g$, total pore volume of 0.82 $cm^3/g$ and average pore diameter of 115 Å are characteristic of the support. The resulting wet catalyst was dried at 110 °C for 8–10 h (sample CoMo(110)). Several catalyst samples were dried in a muffle furnace at temperatures 220, 300 and 400 °C, they were labeled CoMo(220), CoMo(300) and CoMo(400), respectively.

### 2.2. Testing of the hydrotreatment catalysts

A three-phase down-flow reactor (internal diameter 16 mm and isothermal zone 300 mm in length) was used for sulfiding of the catalysts and its testing in hydrotreatment of straight-run gas oil (SRGO). The feed was fed to the reactor using a HPLC pump; hydrogen was portioned using an automated Bronkhorst flow mass. The desired pressure of hydrogen was controlled by back pressure regulator. For each test 10 ml of catalyst granules were mixed with fine carborundum particles (fraction 0.25–0.5 mm) at the ratio 1:1 and loaded in the isothermal zone of the reactor [44]. Carborundum is also loaded below and above the catalyst bed.

Catalysts were sulfided in the reactor by a straight-run gas oil containing extra sulfur (0.6%) as a constituent of dimethyldisulfide (DMDS). The procedure included several steps [39,45,46]:

- Drying in flowing hydrogen at 120 °C for 5 h.
- Wetting the catalyst by the feedstock and increasing hydrogen pressure in the reactor up to 3.5 MPa.
- Temperature elevation up to 230 °C at the rate of 25 °C/h.
- Sulfiding at 230 °C for 5 h (low-temperature stage).
- Temperature elevation up to 340 °C at the rate of 25 °C/h.
- Sulfiding at 340 °C for 8 h (high-temperature stage).

In the course of sulfiding, the flow rate of the sulfiding feed was 2 $h^{-1}$ and hydrogen/oil ratio equaled 300, SRGO being used for preparation of the sulfiding mixture. Transformations of DMDS in the presence of catalysts were studied by following the changes in the concentrations of DMDS and products of DMDS decomposition in the sulfiding mixture, in the concentrations of methane and hydrogen sulfide in the effluent gas at all the steps of sulfiding.

Catalytic properties of the samples were characterized by the residual sulfur content in the straight-run gas oil after the latter was subjected to hydrotreatment at 340 °C, 3.5 MPa, flow rate 2 $h^{-1}$, and hydrogen/oil 300. Properties of the initial SRGO are summarized in Table 1. Residual sulfur content was the average of three samples of hydrotreated product picked up in 10, 11 and 12 h after beginning of each next stage differing by the experimental conditions.

An Agilent 6890N chromatograph equipped with an atomic-emission detector was used for determining sulfur content (with reference to the line of atomic sulfur emission at 181 nm, $S^{181}$ nm) in the hydrotreated product, as well as for quantitative identification of the products of DMDS decomposition in the sulfiding mixture. A capillary chromatographic column HP-1MS (60 m length, 0.32 mm internal diameter, and 0.25 μm thickness film) was used for the separation of components of SRGO at the temperature in the chromatograph thermostat elevated from 40 up to 240 °C at the rate of 2 °C/min and then up to 260 °C at the rate of 10 °C/min.

Liquid feed was sampled for analysis at 30 min intervals. Quantitative analyses were carried out in terms of the areas of the $S^{181}$ nm peaks at retention times of 3.43, 3.60, 3.90, and 6.75 min. These peaks were identified as hydrogen sulfide, methanethiol, dimethylsulfide and DMDS, respectively (Fig. 1).

Concentrations of hydrogen sulfide and methane in the outlet gas were determined using a thermal conductivity detector with hydrogen as gas carrier. The compounds were separated at 120 °C and flow rate of 30 ml/min of the gas carrier in a chromatographic column (2 m length and 2 mm internal diameter) filled with Chromosorbe-104.

### 2.3. Characterization techniques

The atomic adsorption method was used for measuring contents of main components (Co and Mo) in the oxide species of the catalyst. In the sample calcined at 550 °C for 4 h,

**Table 1**
Characteristics of SRGO.

| | |
|---|---|
| Sulfur concentration, ASTM D 4294 (wt%) | 1.104 |
| Total aromatics, IP 391/395 (wt%) | 30.86 |
| Density at 15 °C, ASTM D 4052 (g/ml) | 0.855 |
| Boiling point distribution, ASTM D 2887 (°C) | |
| 10% | 241 |
| 50% | 286 |
| 90% | 341 |

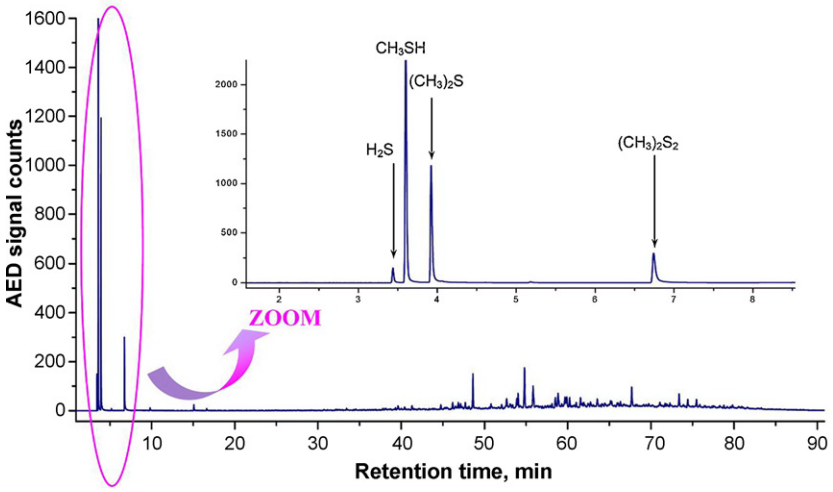


**Fig. 1.** $S^{181}$ chromatogram of sulfiding feed after the contact with a CoMo(300) catalyst (temperature 230 °C, $H_2$ pressure 3.5 MPa, LHSV 2 $h^{-1}$, $H_2$:feed ratio = 300). In the right corner the scaled-up chromatogram in the region of 2–8 min.

concentrations of the active components were 3.85 wt% Co and 11.0 wt% Mo.

Thermal analysis, the thermogravimetric (TG) and differential thermogravimetric (DTG) analysis, of pre-dried samples was conducted using a NETZSCH STA 449C-Jupiter apparatus. TG and DTG curves were recorded in flowing air in the range from room temperature to 600 °C (heating rate 10 °C/min). For analysis, 20 mg of a sample was loaded in a corundum crucible, calcined alumina being used as a reference sample.

The carbon content in the oxidized samples was measured using an element analyzer Vario EL III (ELEMENTAR Analysensysteme GmbH).

Infrared spectra were acquired with resolution 4 $cm^{-1}$ using an IR-Fourier spectrometer BOMEM MB-102 (Canada) in the frequency range 4000–250 $cm^{-1}$. Samples to be characterized were prepared by the standard method by pressing pellets (1.5 mg) of the powder under study mixed with 500 mg of KBr.

The Raman spectra were recorded at room temperature in the range of 3600–100 $cm^{-1}$ using FT-Raman spectrometer RFS 100/S BRUKER (Germany). The used excitation source was the 1064 nm line of Nd-YAG laser operating at power level of 100 mW.

The S/Mo ratio in the sulfided catalysts after they were tested in hydrotreatment of SRGO was XRF determined using a VRA-30 analyzer with a Cr-anode of the X-ray tube.

## 3. Results

### 3.1. Characterization of Co–Mo oxide catalysts precursors

TG and DTG, Raman and IR spectroscopic techniques were used for examining catalysts dried at 110, 220, 300 and 400 °C.

Fig. 2 shows TG and DTG curves of a complex Co and Mo compounds formed by crystallization from the impregnating solution containing ammonia paramolybdate, cobalt acetate and citric acid [43]; Fig. 3 shows the TG and DTG curves of Co–Mo sample thermally treated under different conditions.

As the Co–Mo complex compound is heated, there are observed three ranges of considerable weight losses; these are temperature ranges 50–150, 200–300 and 400–500 °C (Fig. 2). Such a type of DTG curve is characteristic of decomposition of citrate complexes [47–49]. The weight decrease at 50–150 °C is accounted for by releasing adsorbed water. At 200–300 °C citrate ligands are decomposed to the acetonedicarboxylate complexes [47] or oxycarbonate compounds [48]. The weight loss at 400–500 °C accompanied by a noticeable exoeffect usually is attributed to oxidation of the rest fragments of organic molecules [47–49].

In the DTG curves of catalyst samples which have been subjected to thermal treatment at 110, 220, 300 and 400 °C, a considerable weight loss is observed at the temperature range 93–100 °C due to removal of adsorbed water (Fig. 3). In the DTG curve of sample CoMo(110), the weight loss reaches the maximum at 245 °C (10.8% of the total weight of the sample) due to decomposition of citrate ligands in the Co–Mo complex. The presence of this peak is an evidence of the preferable complex localization on the support surface after the impregnation and drying at 110 °C. The DTG peak of weight loss in CoMo(220) related to decomposition of the citrate complex is more broadened with the maximum shifted towards higher temperatures (302 °C), the weight loss being decreased by 4.4%. The broadening indicates the non-uniformity of the decomposed compounds, probably, due to partial or irregular decomposition of the complex treated at 220 °C. In the DTG curve of CoMo(300), the maximum weight loss is observed at 448 °C. It seems that the citrate complex is fully destroyed at 300 °C and carbon species only reside on the surface to be removed at a higher temperature. An only peak assigned to removal of water is observed in the DTG curve of CoMo(400);

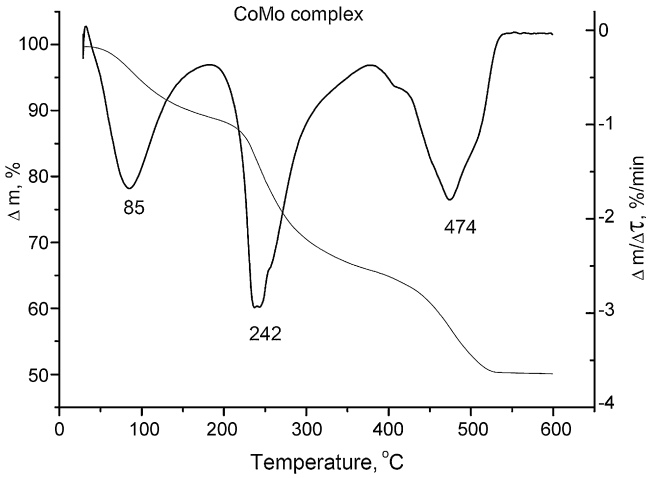


**Fig. 2.** TG and DTG curves of the CoMo complex in the solid state, precipitated from the solution contained ammonia heptamolybdate, cobalt acetate and citric acid [42].

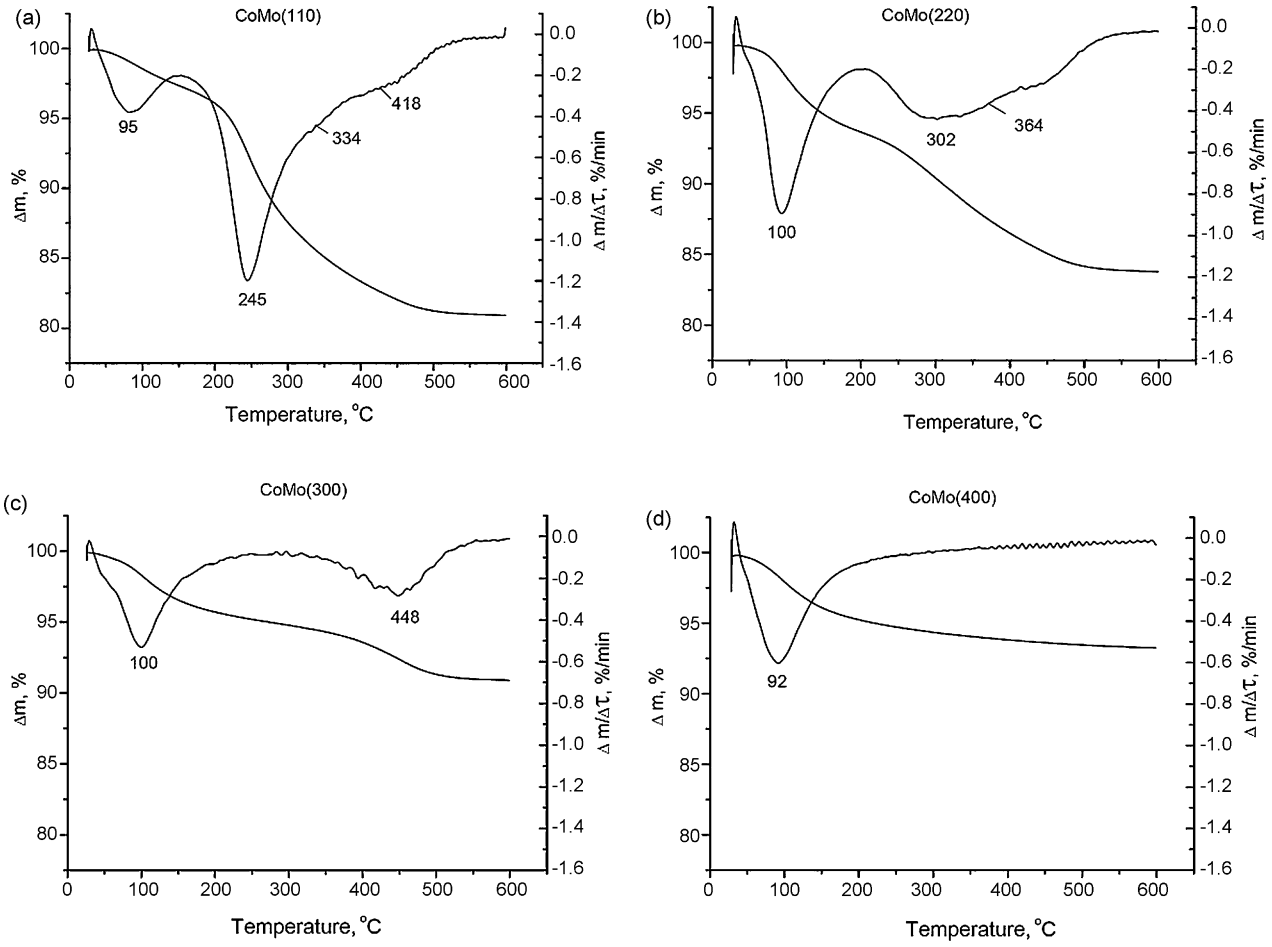


**Fig. 3.** TG and DTG curves of the CoMo catalysts dried at different temperatures: 110 °C (a), 220 °C (b), 300 °C (c), and 400 °C (d).

hence, citrate complexes and products of their decomposition are completely removed during treatment at 400 °C.

The observed phenomena are in good agreement with the data on analysis of carbon obtained using an element analyzer Vario EL III. The carbon content is 5.78, 3.95, 1.79 and 0.05 wt% after thermal treatment at 110, 220, 300 and 400 °C, respectively.

Fig. 4 shows the FTIR spectrum of bimetallic CoMo citrate complex $Co_2[Mo_4(C_6H_5O_7)_2O_{11}]$ formed by crystallization from the impregnating solution containing ammonia paramolybdate, cobalt acetate and citric acid [43]. The structure of bimetallic CoMo citrate complex was characterized using EXAFS and is presented in Fig. 5 [50].

The core of the complex is tetranuclear $[Mo_4(C_6H_5O_7)_2O_{11}]^{4-}$ anion. According to the structural data [51,52], the $[Mo_4(C_6H_5O_7)_2O_{11}]^{4-}$ anion has citrate ligands that contain three non-equivalent carboxylic groups; one is non-bonded and non-dissociated, one is coordinated to molybdenum in a monodentate fashion and the last is bridged to Mo. It was proved that two $Co^{2+}$ cations were coordinated to the Mo-containig anion via two carboxyl groups and the terminal oxygen atom. The bands at 1720–1330 $cm^{-1}$ were assigned to valence vibrations of the carboxyl groups [53]. The vibration modes assigned to the the carboxyl groups bonded with $Co^{2+}$ cations have positions at 1620, 1554 and

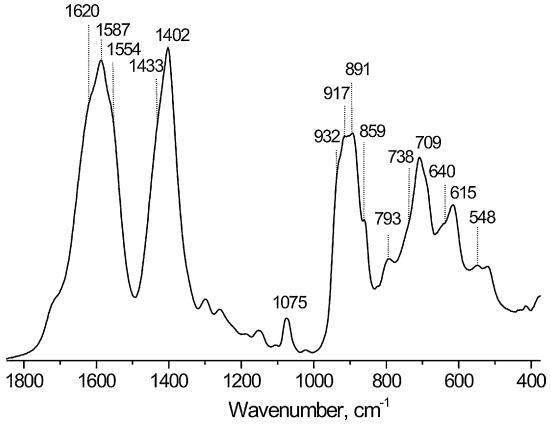


**Fig. 4.** FTIR spectrum for the Co–Mo complex in solid state.

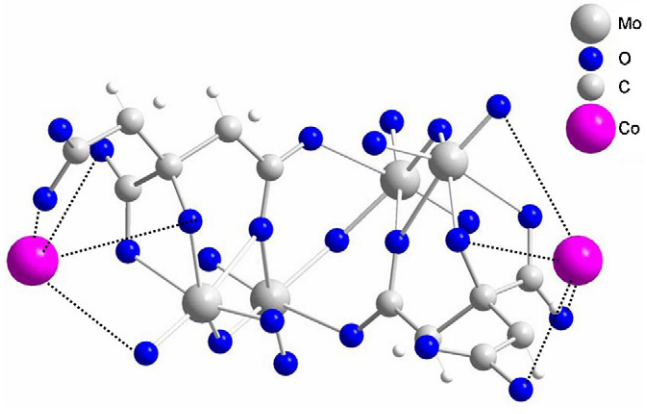


**Fig. 5.** Tentative structure of the bimetallic Co–Mo complex.

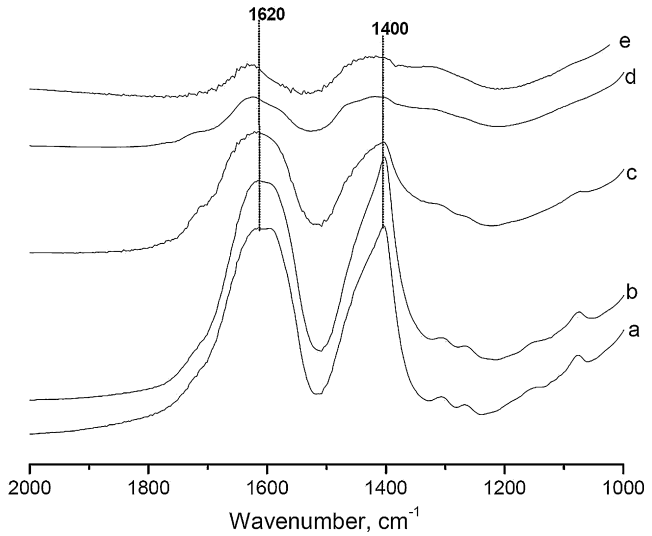


**Fig. 6.** IR spectra in the 1000–2000 $cm^{-1}$ spectral range of CoMo catalysts dried at different temperatures: room temperature (a), 110 °C (b), 220 °C (c), 300 °C (d), and 400 °C (e).

1587 ($\nu_{as}$(COO)) and 1433 and 1402 ($\nu_s$(COO)) $cm^{-1}$, respectively. The latter bands were overlapping with the $\delta_{as}(NH^{4+})$ band. The bands at 960–800 $cm^{-1}$ and 750–520 $cm^{-1}$ were due to valence oscillations of the $MoO_2$ and Mo–O–Mo moieties.

IR and Raman spectra acquired for CoMo samples in the relevant spectral regions are illustrated in Figs. 6 and 7. The IR spectrum of the sample dried at room temperature is in a good agreement with spectrum of unsupported $Co_2[Mo_4(C_6H_5O_7)_2O_{11}]$ complex, two most intense bands (~1620 and ~1400 $cm^{-1}$) in the frequency range 2000–1000 $cm^{-1}$ are corresponded as stated above to asymmetric and symmetric stretching vibrations, respectively, of carboxylic groups of the citrate ligands. Practically identical IR spectra are acquired in this spectra region for

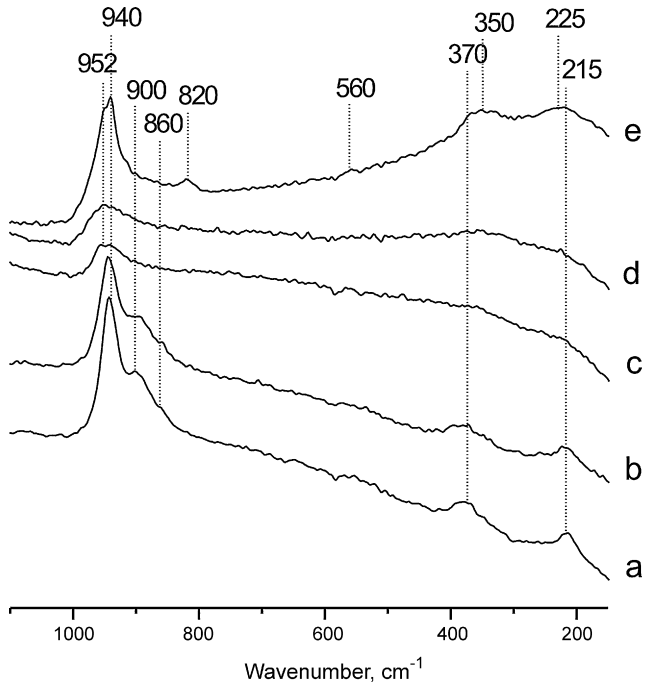


**Fig. 7.** Raman spectra in the 150–1110 $cm^{-1}$ spectral range of CoMo catalysts dried at different temperatures: room temperature (a), 110 °C (b), 220 °C (c), 300 °C (d), and 400 °C (e).

CoMo(110) and for the sample dried at room temperature. In the frequency range 1100–200 $cm^{-1}$ of the Raman spectrum of the latter sample, there are bands at 940, 900, 860, ~370 and 215 $cm^{-1}$ which are assigned, with Ref. [54], to stretching and deformation vibrations of $MoO_{2t}$-fragments. The close similarity of Raman spectra acquired with this sample and with initial complex [43] allows us to assert that the complex preserves its structure on supporting. The Raman spectrum of sample CoMo(110) also is identical to the spectrum of the sample dried at room temperature. Hence, the DTG and spectral data obtained indicate the preservation of the complex structure under conditions of its supporting and drying at 110 °C.

In the IR spectrum of CoMo(220), the bands related to vibrations of citrate ligands are considerably less intense. In the Raman spectrum of this sample, a considerable decrease in the intensity of bands of the initial complex also is observed, while a broad band appears with the maximum at ca. 950 $cm^{-1}$, which may be assigned to surface polymolybdate species [55]. Hence, the calcination of at 220 °C results in partial decomposition of the initial Co–Mo complex.

The bands related to vibrations of citrate ligand are not observed in the IR spectrum of CoMo(300). Low-intense bands at 1720–1200 $cm^{-1}$ here may be assigned to the decomposition products of the citrate ligands (surface carbonate and/or carboxylate species) and adsorbed water. There is one broad band with the maximum at ca. 950 $cm^{-1}$ in the Raman spectrum of this sample; this band is assigned above to surface polymolybdate species. Hence, calcination of the initial sample at 300 °C results in the complete decomposition of the initial complex to form surface polymolybdate compounds.

IR spectra of CoMo(300) and CoMo(400) at the frequency range 2000–1000 $cm^{-1}$ are similar but their Raman spectra are different. The appearance of the intense lines in Raman spectrum of CoMo(400) points out a high uniformity of the supported catalyst due to the formation of the new surface compounds with well-defined structure. There are bands at 952, 940, 820, 350 and 225 $cm^{-1}$ in the Raman spectrum of CoMo(400), which are assigned to vibrations of β-$CoMoO_4$ [38]. More other, the weak band of 567 $cm^{-1}$ could be attributed to the surface heteropolymolybdates $AlMo_6$ or $CoMo_6$ [38,56] with Anderson structure. The intensive bands in the region of 945–950 $cm^{-1}$ are typical for $AlMo_6$ or $CoMo_6$ [57], these bands, apparently, overlapped with the intensive bands at 940 and 952 $cm^{-1}$ of β-$CoMoO_4$ duplet. Thus, the drying procedure performed at 400 °C leads to the total decomposition of the initial CoMo complex to the formation of new surface compounds, presumably including surface polymolybdates, heteropolymolybdates and β-$CoMoO_4$.

### 3.2. Sulfiding of the catalysts

We shall discuss in detail dynamics of variations in the concentrations of DMDS and its transformation products in the sulfiding feed, as well as in concentrations of hydrogen sulfide and methane in the gas phase as functions of temperature and durability of sulfidation with sample CoMo(300) as an example.

A typical chromatogram of sulfur compounds in the sulfiding mixture after it has contacted the catalyst is shown in Fig. 1. Fig. 8 illustrates the dynamics of time-dependent changes in the concentrations of light sulfur-containing components of our interest. These are hydrogen sulfide (3.43 min), methylmercaptan (3.60 min), dimethylsulfide (3.90 min) and DMDS (6.75 min). Intermediate products of DMDS decomposition—methylmercaptan $CH_3SH$ (MM) and methylsulfide $(CH_3)_2S$ (DMS)—are identified in the sulfiding feed after the contact with the catalyst at 230 °C. As the catalyst is sulfided at 230 °C, the DMDS content decreases to disappear by the end of the stage. One hour after the beginning of

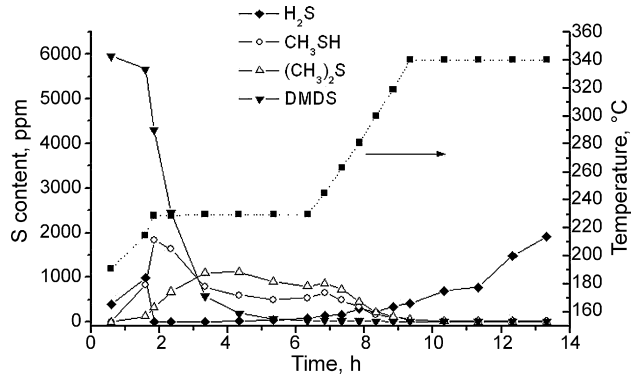


**Fig. 8.** The distribution of the DMDS decomposition products in a liquid phase during the CoMo(300) catalyst sulfidation.

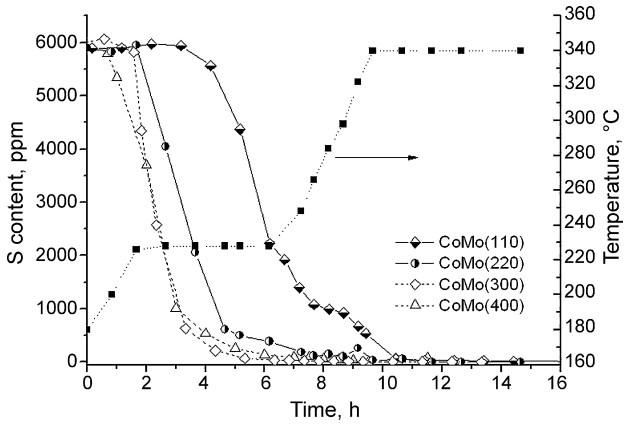


**Fig. 10.** Changes of DMDS concentration during the activation procedure of the CoMo catalysts dried at different temperatures.

the low-temperature sulfiding stage, a peak related to methane appears in the chromatograms, the peak intensity being progressively increased to reach its constant magnitude in another hour (Fig. 9). Detection of methane in the gas phase indicates the complete decomposition of a part of DMDS to produce hydrogen sulfide. Nevertheless, hydrogen sulfide is detected in the chromatograms of the gas phase much later than methane; it is fully consumed for the catalyst sulfiding at the early steps.

On rising the sulfiding temperature from 230 to 340 °C at the next stage, concentrations of the intermediate decomposition products—MM and DMS—decrease; the peaks of these compounds are not visual in the chromatograms of the sulfiding mixture at the temperature above 300 °C. Gas-phase concentrations of methane and hydrogen sulfide increase with temperature. The methane concentration becomes constant at the temperature of ca. 300 °C to indicate the complete decomposition of DMDS and of more stable intermediate products of its decomposition into methane and hydrogen sulfide. These data are in good agreement with the results obtained by analysis of the sulfiding mixture.

Fig. 10 shows the liquid-phase concentration of DMDS depending on temperature and time of sulfiding at different temperatures. There are practically identical curves of DMDS decomposition in the course of sulfiding catalysts CoMo(300) and CoMo(400). The DMDS concentration decreases here to vanish completely by the end of the low-temperature stage. The rate of DMDS decomposition in the presence of CoMo(110) and CoMo(220) becomes noticeable later, the time shift being more considerable with the sample dried at 110 °C. As a result, the DMDS conversion in the presence of this sample is no more than 70% after 5 h reaction of low-temperature sulfiding and approaches to 100% not earlier than the temperature rises up to 340 °C. At the lower catalyst treatment temperature, the later decomposition products (DMS and MM) are detected in the sulfiding mixture.

Time dependencies of gas-phase concentrations of methane and hydrogen sulfide obtained with the samples which were subjected to thermal treatment under different conditions are shown in Fig. 11. Methane is detected in the gas phase the earlier, the higher treatment temperature, the curves of methane generation being practically identical over CoMo(300) and CoMo(400).

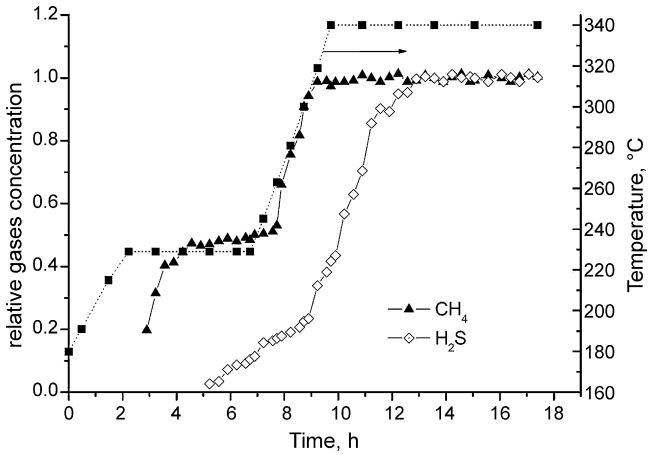


**Fig. 9.** Changes of $CH_4$ and $H_2S$ concentration in a gas phase during the CoMo(300) catalyst sulfidation.

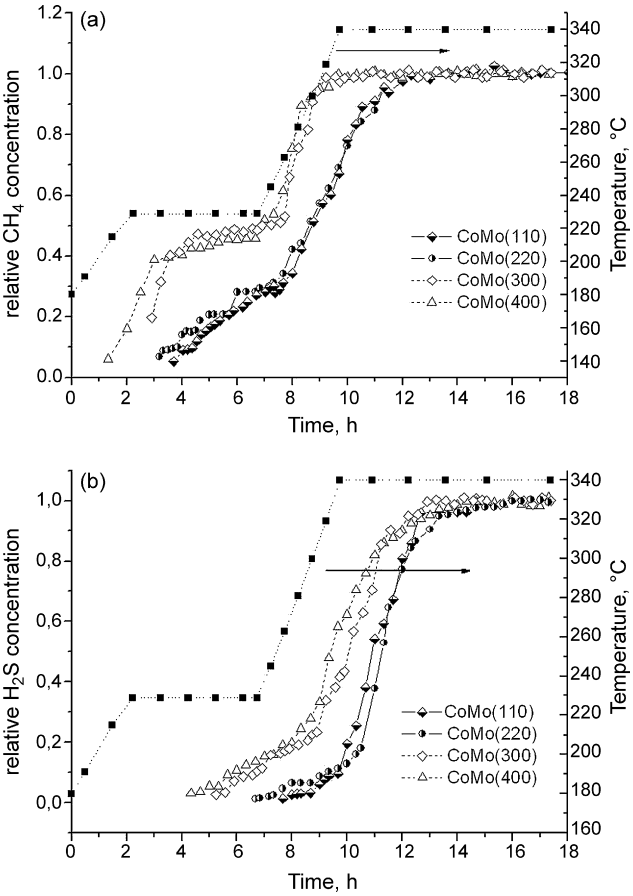


**Fig. 11.** Changes of $CH_4$ (a) and $H_2S$ (b) concentration in a gas phase during the activation procedure of the CoMo catalysts dried at different temperatures.

**Table 2**
Residual sulfur contents after hydrodesulfurization of straight-run gas oil on the CoMO catalysts dried at different temperatures (temperature 340 °C, $H_2$ pressure 3.5 MPa, LHSV 2 $h^{-1}$).

| $H_2$/feed | S content in product (ppm) | | | |
|---|---|---|---|---|
| | CoMo(110) | CoMo(220) | CoMo(300) | CoMo(400) |
| 300 | 69 | 41 | 75 | 104 |
| 200 | 86 | 70 | 98 | 150 |

When the treatment temperature rises from 230 to 340 °C, the gas-phase methane concentration increases in the presence of all the samples. Samples CoMo(300) and CoMo(400) provide the maximal concentration of methane at ca. 300 °C (complete decomposition of DMDS and its transformation products) that agrees with the analytic results on sulfur-containing compounds in the sulfiding mixture (Fig. 10). The maximal gas-phase concentration of methane over CoMo(220) is attained at the sulfiding temperature as high as 340 °C (Fig. 11a). Inspection of curves of gas-phase concentrations of hydrogen sulfide (Fig. 11b) lead us to conclude that hydrogen sulfide becomes detectable in gas phase much later than methane over all the catalysts. The increase in the hydrogen sulfide concentration during catalyst sulfiding became only noticeable at the stage of temperature elevation from 230 to 340 °C over CoMo(300) and CoMo(400) but only at the high-temperature stage at 340 °C over samples CoMo(110) and CoMo(220).

### 3.3. Catalytic activity

Table 2 summaries data on residual sulfur content obtained during hydrotreatment of straight-run gas oil over Co–Mo catalysts prepared under different thermal treatment conditions. The highest activity is seen to be characteristic of CoMo(220). Other catalyst samples under study (the ones treated at 110, 300 and 400 °C) provide higher residual sulfur contents in the hydrotreated product.

## 4. Discussion

Variations in the activity of the $CoMo/Al_2O_3$ catalyst prepared with citric acid as a chelate ligand depending on the thermal treatment temperature can be interpreted based on DTG, IRS and Raman spectroscopy data, as well as on the data on catalyst sulfiding by a mixture of DMDS in gas oil.

Sulfidation is an important stage of the pretreatment of sulfide catalysts for hydrotreatment. This is the stage controlling the active component structure and the catalyst activity. The present vision of the mechanisms of sulfiding Mo-containing catalysts are underlain by studies of sulfiding calcined catalysts with the $H_2S/H_2$ mixture using temperature-programmed sulfidation [58–60], EXAFS [53–61], and Raman spectroscopy [64,65]. In general, the formation of $MoS_2$ particles on the support surface is proceeded through the intermediate compounds—molybdenum oxysulfides [58,59,63–65] or $MoS_3$ [32,60,62]. These compounds start forming at room temperature due to fast O–S exchange between reactive oxygen of molybdenum oxide and sulfur of hydrogen sulfide [58,59,65]. As temperature rises, the intermediates are reduced in the presence of hydrogen to form $MoS_2$; this process usually starts at the temperature above 300 °C. However, at this temperature the sulfiding reaction competes with reduction [45]. For this reason, the catalysts sulfiding needs the formation of intermediate oxysulfide or sulfides at the temperature below 300 °C [34,45].

With dimethyldisulfide, the catalyst sulfiding results from the interaction between the oxide precursors and $H_2S$ or methylmercaptan which are formed by the decomposition of DMDS. The obtained experimental data on decomposition of DMDS over CoMo(300) are illustrated in Figs. 6 and 7; they fit well with the commonly accepted mechanism of DMDS transformations through several stages [45].

Hydrogenolysis of DMDS by reaction (1) produces methanethiol (MM) in the course of a low-temperature stage:

$$CH_3{-}S{-}S{-}CH_3 + H_2 \rightarrow 2CH_3SH \quad (1)$$

In addition, condensation of MM during the low-temperature stage gives dimethyl sulfide (DMS):

$$2CH_3SH \rightarrow CH_3{-}S{-}CH_3 + H_2S \quad (2)$$

Hydrogenolysis of MM on the catalyst surface produces methane and hydrogen sulfide:

$$CH_3SH + H_2 \rightarrow CH_4 + H_2S \quad (3)$$

DMDS also can decompose to generate hydrogen sulfide and methane:

$$CH_3{-}S{-}S{-}CH_3 + 3H_2 \rightarrow 2CH_4 + 2H_2S \quad (4)$$

However the reaction (4) contributes only slightly to the low-temperature decomposition of DMDS [45].

The produced reactants—hydrogen sulfide and methylmercaptan—enter the reaction with the oxide precursors to form gradually a surface sulfide phase which, in turn, starts initiating decomposition of DMDS and MM. Methane appears in detectable quantity in the gas phase shortly after beginning of the low-temperature sulfiding stage. The moment when the peak of gas-phase methane appears can be considered the start of the active decomposition of sulfur-containing compounds with hydrogen sulfide production. Hydrogen sulfide appears much later and in smaller quantity since it is involved in the formation of the active sulfide component and is only detected when the active metal has mainly saturated with hydrogen sulfide.

Thus, CoMo(300) and CoMo(400) catalysts, like the Co–Mo catalysts prepared by traditional methods, provide the following mechanism: decomposition of DMDS starts at 190–200 °C to form MM and hydrogenolysis of DMDS at 230 °C to form methane and hydrogen sulfide [45]. The same mechanism of DMDS transformations is revealed by comparative analysis of variations in the concentrations of DMDS and its transformation products in the presence of CoMo catalysts calcined at different temperatures. However, decomposition of the sulfiding agent and, therefore, sulfidation of the catalysts starts the later, the lower temperature of thermal treatment of the catalyst oxide precursor.

Catalyst characterization results coupled with an on-line analysis of the products formed by the DMDS decomposition during the sulfidation of the samples allow us to interpret the observed effects. From relevant DTG, FTIR and Raman data, the oxide precursors of the active component preserve almost completely the structure of initial CoMo complex with citrate ligands when the sample is dried at 110 °C. When the temperature of the thermal treatment is elevated up to 220 °C, the structure is partly decomposed, while the Co and Mo atoms are surrounded as yet by carbon intermediate which can stabilize them on the support surface.

The stabilization of Co and Mo atoms with citrate ligands results in that they are in the structure of stable compounds in the catalysts dried at the temperature below 220 °C. At the stage of low-temperature activation–sulfidation at 230 °C, carboxylate ligands of the initial complex start decomposing to generate surface Co and Mo compounds which are capable of interacting with the sulfiding agents. The active component is formed simultaneously with the decomposition of citrate ligands thus

providing conditions for more intimate interaction between atoms of the active component (Mo) and promoter (Co) at the sulfidation stage.

DTG and Raman spectroscopic studies demonstrate that the sample calcination at 300 °C or higher temperatures leads to destruction of the complex and formation of the new surface compounds such as surface polymolybdates, heteropolymolibdated, β-$CoMoO_4$ and the products of Mo and Co interaction with alumina occurs. These compounds are easily interacting with the sulfiding agent at a low temperature in much the same way as traditionally prepared calcined Co–Mo catalysts. But it is well known that these surface species are not good precursors for the Co–Mo–S active phase type II [38] and it could not be selectively converted by sulfidation to the active centers of HDS catalysts. This is why CoMo(110) and CoMo(220) are more active than CoMo(300) and CoMo(400).

The obtained results allow us to conclude that influence of drying temperature on the HDS performances of the $CoMo/Al_2O_3$ catalysts prepared using citric acid is rather complicated. Thermal treating conditions determine the structure and composition of the catalyst oxide surface species that in turn influence on sulfidation behavior of the dried catalysts. To correctly activate the catalysts prepared using bimetallic complexes with chelating agent it is essential to exclude high-temperature treatment to avoid the formation of difficult to sulfide surface species and then to provide condition for the oxide precursor transferring into active sulfide phase. Our results agree with the assumption that the preparation of the active catalyst needs the sulfidation under conditions providing the close proximity of Co and Mo atoms (e.g., the presence in the common complex) [30,61]. When the initial complex preserves its structure at the thermal treatment stage, the transformation of the surface oxide compounds into the sulfided form is a slow process, and a lower activity of CoMo(110) in comparison to the activity of CoMo(220) can be accounted for by insufficient saturation of the active component with sulfur at the stage of low-temperature activation. Probably, the active component remains undersulfided in this case. Our assumption is supported by supplementary experimental studies which demonstrated that an increase of the duration of the low temperature sulfidation stage from 5 to 10 h results in a decrease in the residual sulfur content in the hydrotreated product to the level comparable to that in CoMo(220). The retarded sulfidation of the catalysts in which the active components preserve their ligand environment after thermal treatment may be the reason why the calcined catalysts prepared with chelate ligands are more active [36–38]. It is reasonable to suppose that not the conditions of thermal treatment but ineffective sulfidation of the catalysts is responsible for the low activity.

## 5. Conclusion

Experimental data obtained support the opinion reported in literature [6,13,17–22,26,33] that anyone who prepare catalysts using chelate ligand needs to restrict the preparation procedure to the stage of drying in order to provide the higher activity. The present study demonstrate that the temperature of thermal treatment can be different from the traditional drying temperature (100–110 °C) but the complex compound as the active component precursor should be preferably preserved on the support surface. Comparative analysis of regularities of sulfiding the sample treated at different temperatures reveals that the transformation of the surface oxide species into the sulfide form is a slow process when the initial complex preserves its structure during thermal treatment. Hence, the activation of catalysts prepared using chelate ligands needs optimization of the sulfidation procedure to ensure the catalyst saturation with sulfur during the low-temperature stage, for example, by lengthening time or rising temperature at this stage.

## References

[1] S. Eijsbouts, A.A. Battiston, G.C. van Leerdam, Catal. Today 130 (2008) 361.
[2] Technical Regulations, Specification for automotive and aviation gasoline, diesel and marine fuel, fuel for jet engine and burner fuel, Russian Paper 47 (4604) (5 March 2008) 24.
[3] H. Topsøe, B.S. Clausen, Catal. Rev. Sci. Eng. 26 (1984) 395.
[4] H. Topsøe, B.S. Clausen, F.E. Massoth, J.R. Anderson, M. Boudart, Hydrotreating Catalysts in Catalysis: Science and Technology, Vol. 11, Springer, Berlin, 1996.
[5] R. Prins, Hydrotreating reactions, 2nd ed., Handbook of Heterogeneous Catalysis, Vol. 4, VCH Verlagsgesellschaft GmbH, Berlin, 1997.
[6] J.A.R. van Veen, E. Gerkema, A.M. van der Kraan, A. Knoester, J. Chem. Soc., Chem. Commun. 22 (1987) 1684.
[7] J.V. Lauritsen, J. Kibsgaard, G.H. Olesen, P.G. Moses, B. Hinnemann, S. Helveg, J.K. Norskov, B.S. Clausen, H. Topsoe, E. Lægsgaard, F. Besenbacher, J. Catal. 249 (2007) 218.
[8] S.M.A.M. Bouwens, F.B.M. Vanzon, M.P. Vandijk, A.M. Vanderkraan, V.H.J. de Beer, J.A.R. van Veen, D.C. Koningsberger, J. Catal. 146 (1994) 375.
[9] J.A.R. van Veen, H.A. Colijn, P.A.J.M. Hendriks, A.J. van Welsenes, Fuel Proc. Technol. 35 (1993) 137.
[10] J.A.R. van Veen, E. Gerkema, A.M. van der Kraan, P.A.J.M. Hendriks, H.J. Beens, J. Catal. 133 (1992) 112.
[11] H. Topsoe, Appl. Catal. A 322 (2007) 3.
[12] R. Cattaneo, T. Weber, T. Shido, R. Prins, J. Catal. 191 (2000) 225.
[13] Y. Ohta, T. Shimizu, T. Honma, M. Yamada, Stud. Surf. Sci. Catal. 127 (1999) 161.
[14] P. Blanchard, C. Lamonier, A. Griboval, E. Payen, Appl. Catal. A 322 (2007) 33.
[15] K. Inamura, K. Ushikawa, S. Matsuda, Appl. Surf. Sci. 121/122 (1997) 468.
[16] A.J. Van Dillen, R.J.A.M. Terorde, D.J. Lensveld, J.W. Geus, K.P. de Jong, J. Catal. 216 (2003) 257.
[17] T. Shimizu, K. Hiroshima, T. Mochizuki, T. Honma, M. Yamada, Catal. Today 45 (1998) 271.
[18] M. Sun, D. Nicosia, R. Prins, Catal. Today 86 (2003) 173.
[19] E.J.M. Hensen, V.H.J. de Beer, J.A.R. van Veen, R.A. van Santen, Catal. Lett. 84 (2002) 59.
[20] K. Al-Dalama, A. Stanislaus, Energy Fuels 20 (2006) 1777.
[21] S.M.A.M. Bouwens, F.B.M. van Zon, M.P. van Dijk, J. Catal. 146 (1994) 375.
[22] J. Escobar, M.C. Barrera, J.A. de los Reyes, J.A. Toledo, V. Santes, J.A. Colin, J. Mol. Catal. A 287 (2008) 33.
[23] V. Sundaramurthy, A.K. Dalai, J. Adjaye, Catal. Lett. 102 (2005) 299.
[24] M.S. Rana, E.M.R. Capitaine, C. Leyva, J. Ancheyta, Fuel 86 (2007) 1254.
[25] Y. Yoshimura, N. Matsubayashi, T. Sato, H. Shimada, A. Nishijima, Appl. Catal. A. 79 (1991) 145.
[26] T. Fujikawa, H. Kimura, K. Kiriyama, K. Hagiwara, Catal. Today 111 (2006) 188.
[27] T. Fujikawa, Catal. Surv. Asia 10 (2006) 89.
[28] L.G. Pereira, A.S. Araujo, M.J.B. Souza, et al. Mater. Lett. 60 (2006) 2638.
[29] N. Frizi, P. Blanchard, E. Payen, P. Baranek, C. Lancelot, M. Pebeilleau, C. Dupuy, J.P. Dath, Catal. Today 130 (2008) 32.
[30] N. Frizi, P. Blanchard, E. Payen, P. Baranek, C. Lancelot, M. Pebeilleau, C. Dupuy, J.P. Dath, Catal. Today 130 (2008) 272.
[31] A.M. de Jong, V.H.J. de Beer, J.A.R. van Veen, J.W. Niemantsverdriert, J. Phys. Chem. 100 (1996) 17722.
[32] K. Hiroshima, T. Mochizuki, T. Honma, T. Shimizu, M. Yamada, Appl. Surf. Sci. 121/122 (1997) 433.
[33] M.A. Lelias, J. van Gestel, F. Mauge, J.A.R. van Veen, Catal. Today 130 (2008) 109.
[34] L. Medici, R. Prins, J. Catal. 163 (1996) 38.
[35] L. Coulier, V.H.J. de Beer, J.A.R. van Veen, J.W. Niemantsverdriet, Top. Catal. 13 (2000) 99.
[36] Y. Okamoto, S. Ishihara, M. Kawano, M. Satoh, T. Kubota, J. Catal. 217 (2003) 12.
[37] F. Trejo, M.S. Rana, J. Ancheyta, Catal. Today 130 (2008) 327.
[38] P. Mazoyer, C. Geantet, F. Diehl, S. Loridant, M. Lacroix, Catal. Today 130 (2008) 75.
[39] S. Eijsbouts, L.C.A. van den Oetelaar, R.R. van Puijenbroek, J. Catal. 229 (2005) 352.
[40] S. Texier, G. Berhault, G. Perot, F. Diehl, Appl. Catal. A 293 (2005) 105.
[41] A.I. Dugulan, E.J.M. Hensen, J.A.R. van Veen, Catal. Today 130 (2008) 126.
[42] Russian Patent 2312886.
[43] O.V. Klimov, A.V. Pashigreva, M.A. Fedotov, D.I. Kochubey, Yu.A. Chesalov, G.A. Bukhtiyarova, A.S.Noskov, in: Proceedings of the Post-Conference of the 14th International Congress on Catalysis for Ultra Clean Fuels, Dalian, China, July 21–24, 2008.
[44] S.K. Bej, Energy Fuels 16 (2002) 774.
[45] S. Texier, G. Berhault, G. Perot, V. Harle, F. Diehl, J. Catal. 223 (2004) 404.
[46] G. Marroquin, J. Ancheyta, J.A.I. Diaz, Catal. Today 98 (2004) 75.
[47] N.S. Gajbhiye, G. Balaji, Thermochim. Acta 385 (2002) 143.
[48] M. Rajendran, M.S. Rao, J. Mater. Res. 9 (1994) 2277.
[49] L. Bocher, M.H. Aguirre, M. Trottmann, D. Logvinovich, P. Hug, A. Weidenkaff, Thermochim. Acta 457 (2007) 11.
[50] O.V. Klimov, A.V. Pashigreva, D.I. Kochubei, G.A. Bukhtiyarova, A.S. Noskov, Doklady Phys. Chem. 424 (2) (2009) 35.
[51] K. Nakamoto, Infrared and Raman Spectra of Inorganic and Coordination Compounds, John Wiley and Sons, New York, 1986, 536.
[52] N.W. Alcock, M. Dudek, R. Grybos, E. Hodorowicz, A. Kanas, A. Samotus, J. Chem. Soc., Dalton Trans. (1990) 707.

[53] L.R. Nassimbeni, M.L. Niven, J.J. Cruywagen, J.B.B. Heyns, J. Cryst. Spectrosc. Res 17 (1987) 373.
[54] J.A. Bergwerff, T. Visser, B.R.G. Leliveld, B.D. Rossenaar, K.P. de Jong, B.M. Weckhuysen, JACS 126 (2004) 14548–14556.
[55] S. Kasztelan, J. Grimblot, J.P. Bonnelle, E. Payen, H. Toulhoat, Y. Jacquin, Appl. Catal. 7 (1983) 91.
[56] E.N. Yurchenko, The Methods of Molecule Microscopy in the Chemistry of Coordination Compounds and Catalysts, Nayka, Novosibirsk, 1986, p. 256.
[57] C. Martin, C. Lamonier, M. Fournier, O. Mentr, V. Harl, D. Guillaume, E. Payen, Inorg. Chem. 43 (2004) 4636.
[58] B. Sheffer, P.J. Mangus, J.A. Moulijn, J. Catal. 121 (1990) 18.
[59] P. Arnoldy, J.A.M. van den Heijkant, G.D. de Bok, J.A. Moulijn, J. Catal. 92 (1985) 35.
[60] R. Iwamoto, K. Inamura, T. Nozaki, A. Iino, Appl. Catal. A 163 (1997) 217.
[61] D. Nicosia, R. Prins, J. Catal. 231 (2005) 259.
[62] R.G. Leliveld, A.J. van Dillen, J.W. Geus, D.C. Koningsberger, J. Catal. 171 (1997) 115.
[63] N.-S. Chiu, S.H. Bauer, M.F.L. Johnson, J. Catal. 98 (1986) 32.
[64] G.L. Schrader, C.P. Cheng, J. Catal. 80 (1983) 369.
[65] E. Payen, S. Kasztelan, S. Houssenbay, R. Szymanski, J. Grimblot, J. Phys. Chem. 93 (1989) 6501.